

Effects of Thermal Roughening on the Angular Distributions of Trapping and Scattering in Gas–Liquid Collisions

Mackenzie E. King,[†] Kathleen M. Fiehrer,[‡] and Gilbert M. Nathanson*

Department of Chemistry, University of Wisconsin, 1101 University Ave, Madison, Wisconsin 53706-1322

Timothy K. Minton*

Montana State University, Department of Chemistry and Biochemistry, 108 Gaines Hall, Bozeman, Montana 59717

Received: February 28, 1997; In Final Form: May 6, 1997[⊗]

Atomic beam scattering experiments are used to investigate collisions of 71 kJ/mol of argon atoms with perfluorinated polyethers (PFPE) over a wide range of liquid temperatures (T_{liq}) and incident and exit angles. At temperatures ranging from 280 to 359 K, argon atom energy transfer and trapping at the PFPE interface increase steadily with more normal approach directions. Trapping also grows with T_{liq} for all approach and exit directions we measured. The fractional change of trapping with T_{liq} is $2\text{--}5 \times 10^{-3} \text{ K}^{-1}$, rising weakly with more grazing impact angles. In contrast, the inelastic scattering flux decreases with increasing T_{liq} at forward scattering angles and increases for backward deflections. These results are consistent with a surface of protruding hard sphere-like CF_x groups that becomes more corrugated at higher temperatures, promoting multiple collisions of incoming atoms at all impact angles.

Introduction

Energy dissipation in collisions between gas atoms and molecular liquids depends on many aspects of the encounter, including the impact energy and approach direction of the gas atom and the packing and orientation of molecules at the liquid's surface. Angle- and energy-resolved studies¹ of rare gas collisions with squalane ($\text{C}_{30}\text{H}_{62}$) and a perfluorinated polyether (PFPE) revealed two limiting types of encounters: direct inelastic scattering (IS) and trapping–desorption (TD).^{2,3} Atoms in the IS channel scatter impulsively from the surface in one or a few bounces, transferring only a fraction of their energy to the liquid phase molecules before recoiling from the interface. Atoms in the TD channel instead spend enough time in contact with the surface to dissipate their incident energy and become temporarily bound. These trapped atoms then desorb from the interface, propelled into the vacuum by thermal motions of the surface molecules. These studies also showed that the IS channel obeys a deflection rule: energy transfer during an inelastic collision depends uniquely on the angle of deflection, $\chi = 180^\circ - \theta_i - \theta_f$, where θ_i and θ_f are the incident and exit angles, respectively.⁴ For an atom with incident energy E_i , the fractional energy transfer $\langle \Delta E_{\text{IS}} \rangle / E_i$ increases steadily with χ , as predicted by hard sphere-like collisions between the gas atom and protruding CH_x and CF_x groups at the interface.

The angle-resolved studies were followed by fixed-angle experiments exploring how inelastic scattering and trapping–desorption vary with the temperature of the liquid, T_{liq} .⁵ At $\theta_i = \theta_f = 45^\circ$, trapping and desorption of high-energy atoms grew at the expense of direct inelastic scattering as the PFPE liquid was heated. These results suggested that thermal motions enhance the roughness of the PFPE surface, causing some incoming atoms that would have scattered directly at lower temperatures to undergo multiple deflections within the interface and become accommodated before departing.

The fixed-angle experiments raised several questions regarding the role of thermal motions in gas–liquid energy transfer and accommodation. Is the observed drop in inelastic scattering with higher T_{liq} due just to a shift in the direction of the recoiling atoms and not from an overall conversion of impulsive scattering into trapping–desorption? More generally, how do the IS and TD fluxes vary with impact and exit directions as the liquid is heated? Is there evidence that thermal motions at the interface can reorganize the PFPE chains into trapping atoms preferentially along specific approach directions?

We chose the PFPE Krytox 1625, $\text{F}[\text{CF}(\text{CF}_3)\text{CF}_2\text{O}]_{27(\text{ave})}\text{CF}_2\text{CF}_3$, to address these questions because its vapor pressure is low over the accessible temperatures in our experiments from 280 K ($\approx 3 \times 10^{-11}$ Torr) to 359 K ($\approx 1 \times 10^{-6}$ Torr).⁶ Over this temperature range, the viscosity of Krytox 1625 drops from 1500 to 30 cP. The fluid has a high mass density that drops from 1.92 to 1.77 g/cm^3 over the 79 K interval, corresponding to a 9% increase in volume. These high liquid densities lead to low inelastic energy transfers, allowing a cleaner separation of the IS and TD components in the time-of-flight (TOF) spectra.¹ The perfluorinated chains are stiffer than hydrogenated alkyl ethers, and they are bound by weak intermolecular forces corresponding to ≈ 5 kJ/mol per monomer.⁶ The carbon–fluorine bonds impose low surface tensions, ranging from 19.4 to 15.6 mN/m from 280 to 359 K. Recent sputtering and photoelectron studies of Krytox fluids indicate that the CF_3 chain ends poke out at the surface and that the O atom linkages are buried deeper into the interface.⁷

We report below angle-resolved scattering studies of 71.5 kJ/mol of argon atoms colliding with Krytox 1625 between 280 and 359 K that provide preliminary answers to the questions raised above. Argon was chosen as the impinging gas because it is the smallest and lightest atom for which the IS and TD channels are each substantial and distinguishable. The data show that argon atom energy transfer and trapping is always favored at more normal than more grazing incidence. We also observe that the fractional change in trapping with temperature is always positive, and that it is slightly greater for glancing

[†] Present address: ATMI, 7 Commerce Dr., Danbury, CT 06810.

[‡] Present address: Intel Corporation, 5200 N. E. Elam Young Parkway, Hillsboro, OR 97124.

[⊗] Abstract published in *Advance ACS Abstracts*, July 15, 1997.

collisions than for normal approach angles. In contrast, inelastic scattering decreases with temperature at forward scattering angles and increases with T_{liq} for backward deflections. The results indicate that thermally induced surface roughening accelerates the approach to gas–liquid equilibrium for all directions of the incoming gas atoms.

Experiment

The experiments were performed with a scattering machine equipped with a rotating mass spectrometer. The mass spectrometer and liquid surface rotate about the same plane so that intensities and arrival times of the exiting atoms can be monitored as a function θ_i and θ_f within the scattering plane. The final translational energies, E_f , of argon atoms scattering from the PFPE liquid are determined by recording their flight times over the 30.4 cm distance between the mass spectrometer and a 150 Hz chopper wheel with four 1.6 mm wide slots.

Clean and continuously renewed films of PFPE are prepared using the methods of Lednovich and Fenn.⁸ A 5.4 cm diameter wheel, partially submersed in 37 mL of Krytox 1625, drags a thick liquid film upward as it rotates at 0.25 Hz. A 0.25 mm thick sapphire plate scrapes away surface impurities and leaves a fresh 0.14 mm thick liquid layer in the interaction zone. T_{liq} is regulated between 280 and 359 K to within $\pm 0.1^\circ$ over the 3 min TOF measurements. Atomic beams of argon are generated by expanding Ar seeded in H_2 at 158 Torr through a 0.11 mm diameter tapered glass nozzle held at 333 K. The incident energy is 71.5 ± 22.1 kJ/mol (full width at half-maximum).

The TOF spectra are recorded twice at each angle at 280, 303, 331, and 359 K at $m/e = 40$. No evaporating background from PFPE was detected at this mass. The range of incident and exit angles varies from $\theta_i = 0^\circ$ to 65° and $\theta_f = -18^\circ$ to 70° , under the constraint that $\theta_i + \theta_f \geq 47^\circ$. The signal intensity is reproducible to within 3% over an 8 h recording period. All spectra have been corrected for electronic and ion flight time offsets.

Results and Analysis

Time-of-Flight Analysis. The TOF spectra are plots of number density, $N(t, \theta_i, \theta_f, T_{\text{liq}})$, versus arrival time t . The spectra are used to compute the relative fluxes or intensities, $I(E_f, \theta_i, \theta_f, T_{\text{liq}})$, of the scattered argon atoms from the relation $I(E_f) \propto N(t)t^2$, where $E_f = (1/2)m_{\text{gas}}(L/t)^2$ and $L = 30.4$ cm. These intensities are proportional to the relative probability, $P(E_f)$, that an argon atom will scatter from PFPE at final energy E_f . The trapping–desorption channel is assigned to those exiting atoms which fall within a Boltzmann distribution at T_{liq} , such that $I_{\text{TD}}(E_f) \propto [E_f/(RT_{\text{liq}})^2]e^{-E_f/RT_{\text{liq}}}$.⁹ The inelastic scattering channel is set equal to the difference between the total and TD distributions. This subtraction is fixed by assuming that $I_{\text{IS}}(E_f) = 0$ at $E_f = RT_{\text{liq}} = 2.3\text{--}3.0$ kJ/mol. We also compute the integrated intensities, $I(\theta_i, \theta_f, T_{\text{liq}}) \propto \int (N(t)/t) dt$, which yield the relative fluxes of atoms scattering from θ_i into θ_f at T_{liq} . The analysis of the TOF spectra is facilitated by direct inversion without convolution over the 40 μs opening time of the chopper wheel. This inversion overestimates the flux-averaged energy by $<1\%$ and underestimates the TD flux by $<1\%$.

Figure 1 shows the fitting procedure for argon striking PFPE at $\theta_i = \theta_f = 45^\circ$ and at $T_{\text{liq}} = 331$ K. The $N(t)$ and $P(E_f)$ distributions are each split into TD and IS components. The average recoil energy in the IS channel is 31.7 kJ/mol, yielding an average energy transfer of 0.56 for inelastically scattered atoms at $\theta_i = \theta_f = 45^\circ$. Figure 1b also shows that the IS

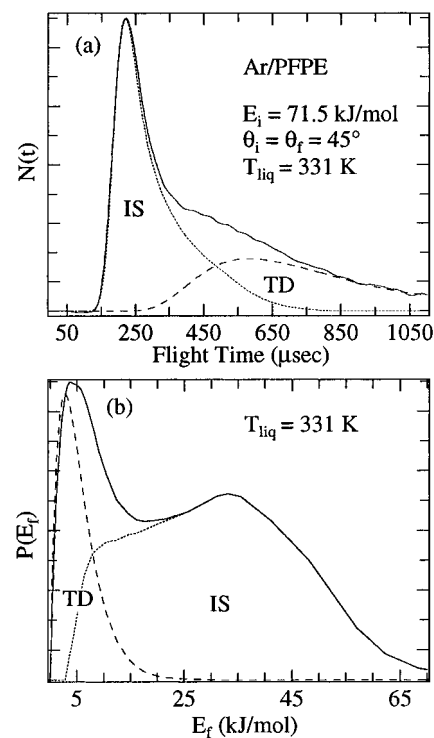


Figure 1. (a) Time-of-flight spectrum of 71.5 ± 22.1 kJ/mol of argon scattering from a perfluorinated polyether and (b) translational energy distribution determined from the TOF spectrum. IS and TD label the direct inelastic scattering and trapping–desorption components.

channel has a shoulder at low exit energies. This low-energy scattering has been observed previously in rare gas collisions with PFPE⁵ and with the atomic liquids indium and gallium,¹⁰ where it was attributed to atoms undergoing two or more collisions with large deflection angles and consequent extensive energy loss.¹¹

We attempted to reduce the size of the shoulder and fit the low-energy peak entirely within the TD channel by using a floating temperature instead of T_{liq} in $I_{\text{TD}}(E_f)$. The resulting temperatures were over 100 K hotter than T_{liq} and varied strongly with θ_f . We note that at large $\theta_i + \theta_f$, where the IS and TD peaks are better separated, the floating temperatures are within 30 K of T_{liq} .¹² The floating-temperature fits also yield TD intensities that are highly nonsymmetric about $\theta_f = 0^\circ$, in contrast to the requirement that trapped atoms lose memory of their initial approach direction. These results lead us to believe that the higher energy side of the low-energy peak in Figure 1b is composed of inelastically scattered atoms undergoing extensive energy loss¹³ and that the decomposition using $T = T_{\text{liq}}$ is more correct. T is set equal to T_{liq} in the data analysis below.

Changes in TOF Spectra with T_{liq} , θ_i , and θ_f . Figure 2 shows TOF spectra of 71.5 ± 22.1 kJ/mol of Ar scattering from PFPE at $\theta_i = 0^\circ, 25^\circ, 45^\circ$, and 65° for a fixed observation angle of $\theta_f = 45^\circ$. The spectra were recorded at $T_{\text{liq}} = 280$ K in the upper panel and at 359 K in the lower panel. The IS, TD, and total intensities, integrated over E_f , are displayed in Figure 3 as a function of θ_i and T_{liq} . Figures 2 and 3 illustrate three features.

(1) At fixed exit angle and liquid temperature, the TD flux decreases as the approach direction is varied from perpendicular to glancing impact (increasing θ_i). Over the range $\theta_i = 0\text{--}65^\circ$, the TD flux drops by factors of 2.4 and 2.1 at 280 and 359 K, respectively. These ratios are reproduced to within ± 0.2 at exit angles of $\theta_f = 25^\circ$ and 70° .

(2) The IS channel shifts to higher recoil energies (shorter arrival times) and larger intensities as θ_i increases. The IS intensities grow by a factor of 1.8 as θ_i increases from 0° to

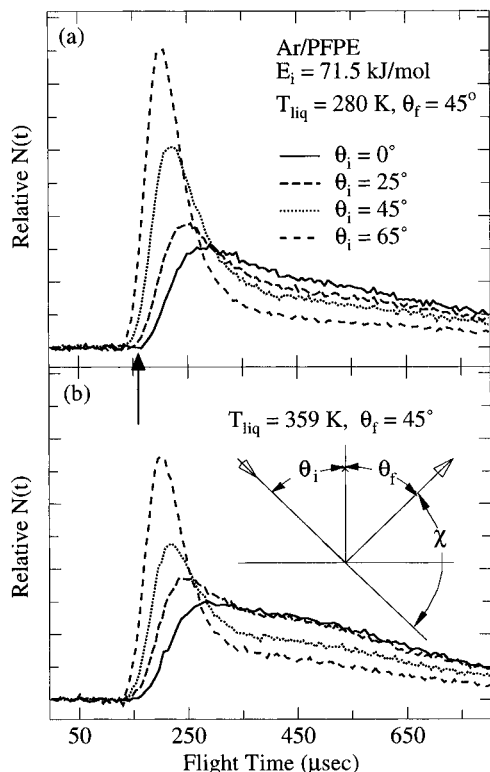


Figure 2. TOF spectra of argon scattering from PFPE at incident angles $\theta_i = 0^\circ$, 25° , 45° , and 65° for a fixed detection angle of $\theta_f = 45^\circ$ (except for $\theta_i = 0^\circ$, where $\theta_f = 47^\circ$). The vertical arrow points to the peak arrival time of elastically scattered atoms. (a) Liquid temperature = 280 K. (b) Liquid temperature = 359 K.

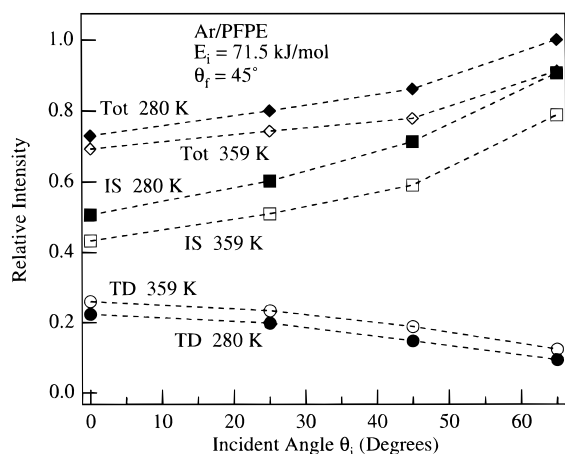


Figure 3. Trapping–desorption (TD), inelastic scattering (IS), and total intensities integrated over all arrival times for the TOF spectra in Figure 2. The filled and open symbols refer to liquid temperatures of 280 and 359 K, respectively.

65° at both 280 and 359 K. This ratio jumps to ≈ 3.5 for $\theta_f = 70^\circ$ and is closer to one at $\theta_f = 25^\circ$.

(3) At fixed θ_i and for $\theta_f = 45^\circ$, the IS fluxes decrease and the TD fluxes increase as the liquid is heated. The overall flux also decreases with T_{liq} when monitored at $\theta_f = 45^\circ$. A detailed analysis of this temperature dependence is presented below.

The inelastic scattering flux does not always drop as the temperature is increased. Figure 4 shows TOF spectra of argon scattering at $\theta_i = 65^\circ$ for backward scattering at $\theta_f = -18^\circ$ and forward scattering at $\theta_f = +30^\circ$. The IS signal increases with T_{liq} at $\theta_f = -18^\circ$, while it drops at $\theta_f = +30^\circ$. We do not yet know if the growth in IS flux with T_{liq} shown in the top panel also occurs at more extreme backward deflections. The

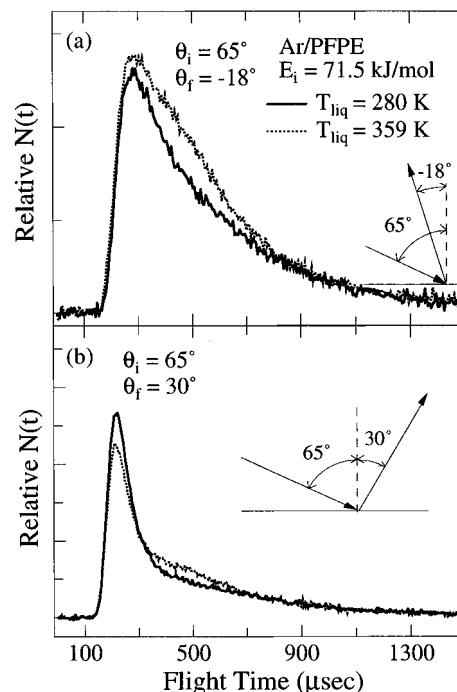


Figure 4. Argon scattering from PFPE at 280 and 359 K at $\theta_i = 65^\circ$ and (a) $\theta_f = -18^\circ$ and (b) $\theta_f = 30^\circ$.

decrease in IS intensity with T_{liq} in the bottom panel is typical of forward scattering greater than $\theta_f = 10^\circ$. Figure 4 also illustrates that the TD flux grows with increasing T_{liq} in both spectra, as it does at all incident and exit angles we measured.

Figure 5 shows how the PFPE temperature alters the TD, IS, and total intensities as a function of exit angle at fixed $\theta_i = 65^\circ$. Panel (a) compares the TD fluxes with best-fit cosine distributions (which are expected for thermal desorption when the trapping probabilities are independent of θ_i at thermal energies,³ from $E_i = 0$ to ≈ 15 kJ/mol). The intensities do increase as θ_f drops from 70° to 0° , but they do not turn over at negative (backscattering) angles up to -18° . As described above, this lack of azimuthal symmetry is likely caused by low-energy inelastic scattering that was not fully subtracted from the TOF spectra at backward deflection angles.¹³ The IS intensities were then corrected by imposing azimuthal symmetry on the TD distribution. These corrected intensities are shown in panel (b) by the dashed and dotted lines. The corrections are small: for both the original and azimuthally constrained data, the IS intensities increase with θ_f until they turn over near 60° . The inelastic scattering flux in each case is higher at 359 K than at 280 K at negative angles, crossing at $\theta_f = 10^\circ$. The temperature dependence of the total intensity shown in panel (c) reflects the competition between the IS and TD channels, yielding a crossover between the 280 and 359 K curves at θ_f near 30° .

The intensities at all four temperatures are displayed in Figure 6 for $\theta_i = 65^\circ$ and $\theta_f = -18^\circ$, 30° , and 70° . Panel (a) shows that the TD flux grows at each exit angle as the liquid is heated. The TD flux is weakest at $\theta_f = 70^\circ$, as expected from the angular distribution in Figure 5. The IS flux shown in panel (b) is largest at glancing angles, where the energy transfer is smallest. It decreases with T_{liq} for both forward scattering angles and increases slightly with T_{liq} at $\theta_f = -18^\circ$. The total intensity shown in panel (c) largely mirrors the trends in the IS channel.

The final results are plotted in Figure 7, which displays the fractional changes in intensity, $(1/\langle I \rangle)\Delta I/\Delta T_{\text{liq}}$, versus θ_f . These fractional changes reveal how the liquid's temperature affects the scattering probability as a function of impact and exit angles.

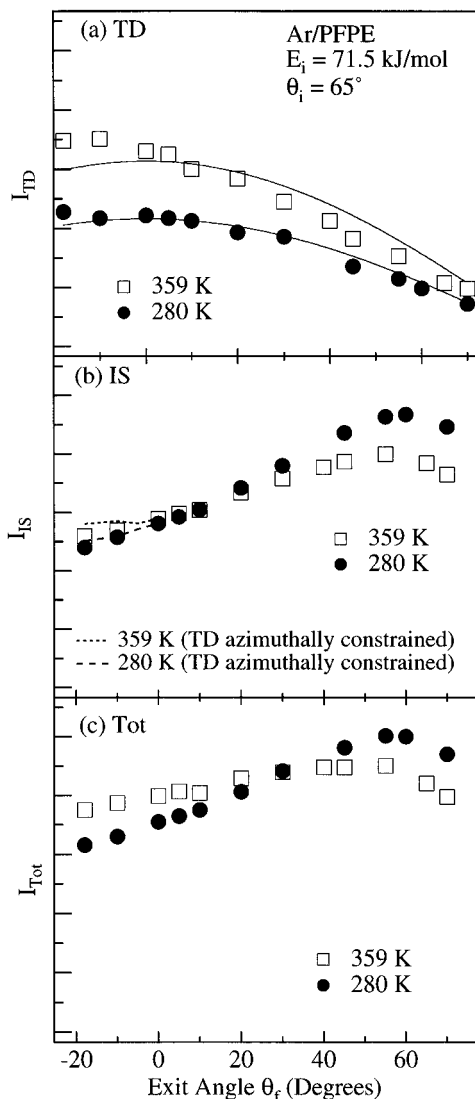


Figure 5. TD, IS, and total (Tot) intensities for liquid temperatures of 280 and 359 K at $\theta_i = 65^\circ$. In panel (a), the TD intensities are multiplied by 3.0 relative to those of the IS and total intensities. In panel (b), the dashed and dotted lines display the IS intensities at negative θ_f when the TD distribution is constrained to be symmetric about $\theta_f = 0^\circ$.

The error bars represent $\pm 2\sigma$, based on a least-squares analysis of the slopes in Figure 6 and similar plots. The fractional changes in TD intensity are on the order of $2-5 \times 10^{-3} \text{ K}^{-1}$. To obtain better statistics, we make the assumptions that trapping and desorption are separate events and that the desorption angular distributions are independent of temperature. The intensity $I_{TD}(\theta_i, \theta_f, T_{liq})$ can then be factored into $g(\theta_i, T_{liq}) h(\theta_f)$ and the fractional change $(1/\langle I_{TD} \rangle) \Delta I_{TD} / \Delta T_{liq}$ equals $(1/\langle g \rangle) (\Delta g / \Delta T_{liq})$, independent of θ_f . In this ideal case, we can average the values of $(1/\langle I_{TD} \rangle) \Delta I_{TD} / \Delta T_{liq}$ at different θ_f , since they are repeated measurements of the same quantity.¹⁴ The averages over all recorded exit angles are $(1/\langle I_{TD} \rangle) \Delta I_{TD} / \Delta T_{liq} = 4.2 \pm 0.5 \times 10^{-3} \text{ K}^{-1}$ for $\theta_i = 65^\circ$ and $3.0 \pm 0.3 \times 10^{-3} \text{ K}^{-1}$ for $\theta_i = 45^\circ$ (90% confidence intervals). The ratio of these values is 1.4 ± 0.2 . The average TD fractional changes for $\theta_i = 0^\circ$ and 25° are $\approx 2.0 \times 10^{-3} \text{ K}^{-1}$ if the values at $\theta_f = 70^\circ$ are excluded. The average values at $\theta_i = 0^\circ$ and 25° are less certain than those at 45° and 65° because fewer data points were recorded and because of the difficulty in separating the IS and TD components for these spectra.

The fractional changes in IS intensity are small but positive for backscattering directions and become negative for forward scattering directions. The IS values are similar for all measured

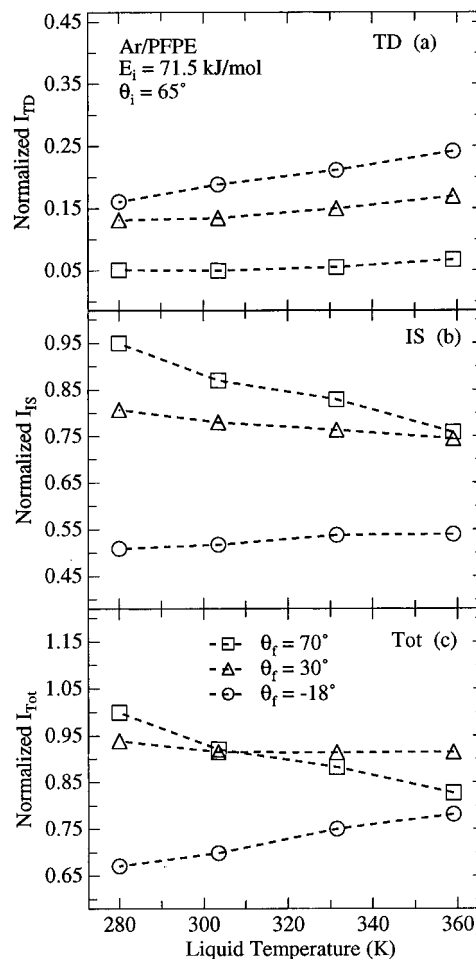


Figure 6. TD, IS, and total intensities versus liquid temperature for $\theta_i = 65^\circ$ and $\theta_f = -18^\circ$ (○), $\theta_f = 30^\circ$ (△), and $\theta_f = 70^\circ$ (□). Each intensity is normalized to I_{Tot} (280 K, $\theta_f = 70^\circ$).

impact angles at $\theta_f = 45-70^\circ$, falling between -2 and $-3 \times 10^{-3} \text{ K}^{-1}$, and are nearly equal in magnitude to the TD values recorded at $\theta_i = 45^\circ$.

Discussion

Figures 3 and 7 summarize the relative rates of trapping–desorption and inelastic scattering as a function of impact angle and temperature for collisions of hyperthermal argon atoms with liquid PFPE. At fixed T_{liq} , trapping is always favored at more normal approach angles. The fractional changes in trapping with T_{liq} , $(1/\langle I_{TD} \rangle) \Delta I_{TD} / \Delta T_{liq}$, are always positive and appear to increase weakly but steadily with more glancing impact. The inelastic flux compensates by decreasing with increasing T_{liq} , at least at forward scattering angles.

Trapping versus Approach Angle. The increase in trapping with more normal approach angles is expected for hard sphere-like collisions between inert gas atoms and the protruding CF_x segments of PFPE along a macroscopically flat surface. More normal approach angles lead both to greater energy transfers during the initial collision and more collisions per encounter.^{15,16} At grazing incidence, atoms may often strike the top regions of the protruding groups and deflect only slightly as they scatter in forward directions with small energy losses.¹⁷ For perpendicular approach, atoms which initially scatter away from the surface must be deflected by 90° or more and lose a substantial fraction of their energy,¹ while those deflected toward the liquid undergo at least one more collision. Atoms deflected inward or along the interface are likely to undergo multiple collisions,

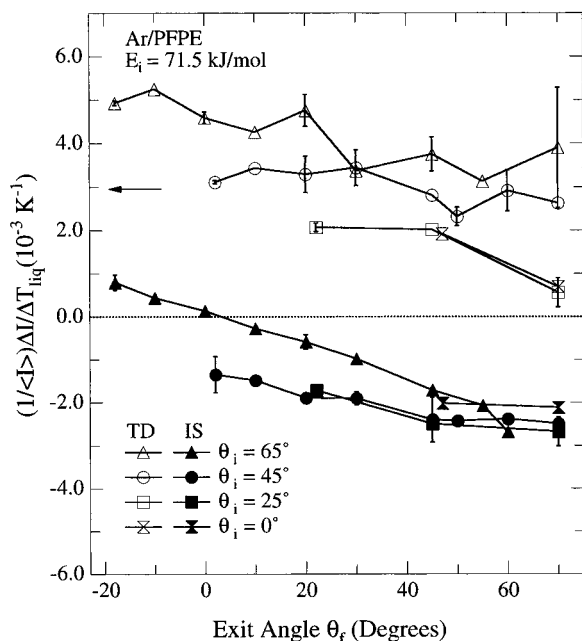


Figure 7. Fractional changes in intensity with liquid temperature in units of 10^{-3} K^{-1} as a function of exit angle. The open and filled symbols refer to $(1/\langle I_{\text{TD}} \rangle)(\Delta I_{\text{TD}}/\Delta T_{\text{liq}})$ and $(1/\langle I_{\text{IS}} \rangle)(\Delta I_{\text{IS}}/\Delta T_{\text{liq}})$, respectively. The error bars represent $\pm 2\sigma$, derived from the least-squares analysis of the slopes $\Delta I/\Delta T_{\text{liq}}$. The horizontal arrow at $3 \times 10^{-3} \text{ K}^{-1}$ is the prediction based on equation 1.

enhancing the chances that the atoms will loose enough energy to be momentarily bound at the surface.¹⁸

Figure 3 shows that the ratio $I_{\text{TD}}(0^\circ)/I_{\text{TD}}(65^\circ)$ lies between 2.1 and 2.4 and that $I_{\text{TD}}(45^\circ)/I_{\text{TD}}(65^\circ)$ is 1.5–1.6. In our previous studies of 81 kJ/mol of Ar and 185 kJ/mol of Xe collisions with PFPE and squalane (Squ) at $T_{\text{liq}} = 290 \text{ K}$, we recorded ratios of $I_{\text{TD}}(45^\circ)/I_{\text{TD}}(65^\circ)$ equal to 1.4 (Ar, PFPE), 1.6 (Ar, Squ), 1.7 (Xe, PFPE), and 1.3 (Xe, Squ).¹ Thus, the argon/PFPE system investigated here may be typical of heavy rare gas collisions with nonreactive oligomeric liquids. It is not representative of reactive gas–liquid collisions where the attractive forces are strong and trapping is irreversible. For example, the reactive uptake of dimethyl ether in 98.8 wt % sulfuric acid at $E_i = 86 \text{ kJ/mol}$ and $T_{\text{liq}} = 295 \text{ K}$ drops by only 10% from $\theta_i = 0^\circ$ to 45° ,¹⁹ while the trapping probabilities in the Ar/PFPE system drop by 40% over the same angular range. The trends, however, remain the same for all gas–liquid systems we have explored: energy transfer and accommodation increase at least weakly as θ_i decreases toward 0° , indicating that interfacial trapping and subsequent solvation are more likely when the gas species approach the surface at more normal approach angles.

Trapping and Inelastic Scattering versus T_{liq} . The data in Figure 7 extend our previous studies⁵ at fixed $\theta_i = \theta_f = 45^\circ$ by demonstrating that trapping rates increase slowly but steadily with the temperature of the liquid over a wide range of incident angles. They also reveal that backscattering is more likely at higher temperatures, as might be expected for a rougher surface. This increase in inelastic scattering at small negative angles is likely accompanied by increasing out-of-plane scattering as well.²⁰

The larger trapping probabilities at higher T_{liq} are consistent with scattering from a rougher interface created by CF_3 groups poking out and burrowing inward, which can deflect atoms along the surface and enhance energy transfer through multiple collisions with protruding end groups. This picture is supported by simulations²¹ of long chain hydrocarbons (Figure 10 of ref

5), which show that the depth and number of gaps and protrusions at the surface grow with T_{liq} . The values of $(1/\langle I_{\text{TD}} \rangle)\Delta I_{\text{TD}}/\Delta T_{\text{liq}}$ in Figure 7 cluster near $(2-5) \times 10^{-3} \text{ K}^{-1}$, increasing at larger θ_i : this trend suggests that thermal roughening of the PFPE interface enhances trapping slightly more at grazing incidence than at normal impact. The enhancement may be due to glancing collisions with CF_3 chain ends poking out further into the vacuum at higher temperatures. These collisions would deflect the incoming atoms backward or out of plane before they could strike a smoother patch of the surface. In particular, they should increase the IS intensity at negative angles, as observed in Figure 4a.

It is possible to estimate the average fractional change in trapping with T_{liq} with a primitive model which connects scattering intensities and the surface roughness, δ . In a previous study of 42 kJ/mol of argon scattering from the atomic liquids indium and gallium, we observed that I_{IS} decreases as the liquids were heated (no trapping–desorption was observable).¹⁰ The data could be fit by expressing the intensity as $I_{\text{IS}} \propto \delta^\alpha$, assuming that most of the surface roughness is caused by small amplitude, thermally induced fluctuations and that $(1/2)k\delta^2 = (1/2)k_{\text{B}}T_{\text{liq}}$. The spring constant k should vary linearly with the surface tension γ ,²² and we obtain

$$(1/\langle I \rangle)\Delta I/\Delta T_{\text{liq}} = \alpha [1/(2\langle T_{\text{liq}} \rangle)] [1 - (\langle T_{\text{liq}} \rangle / \langle \gamma \rangle) (d\gamma/dT_{\text{liq}})] \quad (1)$$

Equation 1 predicts the fractional rate of decrease of inelastic argon scattering from liquid indium and gallium to within 18% and 3%, respectively, for experimentally determined values of $\alpha = -1.04$ (Ga) and -1.1 (In). Equation 1 should also be applicable to the rate of increase of trapping–desorption as well, since some atoms that would have scattered directly at lower T_{liq} now undergo more collisions, enhancing both low-energy backward deflections and the complete energy transfer required for trapping. We have measured the surface tension of PFPE to be $\gamma(T)(\text{mN/m}) = 19.5 - 0.0483(T - 278 \text{ K})$. Using a value of $\alpha = +1$, eq 1 predicts that $(1/\langle I_{\text{TD}} \rangle)\Delta I_{\text{TD}}/\Delta T_{\text{liq}} = 0.0030$ at $\langle T_{\text{liq}} \rangle = 320 \text{ K}$. This value is shown as an arrow in Figure 7, in comparison to an average value of 0.0036 for $\theta_i = 45^\circ$ and 65° . The two values differ by only 20%, and the prediction is close to the average fractional decrease in inelastic scattering at forward angles as well. These similarities suggest that eq 1 may be useful in estimating changes in inelastic scattering and trapping–desorption upon heating liquids as diverse as molten metals and oligomeric fluorocarbons.

Conclusions

The rate of trapping of hyperthermal argon atoms in collisions with perfluorinated ethers increases with more normal impact direction and with the temperature of the liquid. This trend is robust over a wide range of approach directions and liquid temperatures. To compensate for the increase in trapping–desorption, the rate of inelastic scattering must decrease with liquid temperature: we observe this decline in forward scattering directions, but the inelastic scattering flux increases at small backward deflection angles. These observations are consistent with the notion that liquid surfaces are rougher at higher temperatures, deflecting atoms into and along the interface and increasing the number of gas–liquid collisions.

Scattering studies of collisions between organic gases and hydrogen-bonding⁹ and acidic¹⁹ liquids indicate that the rate of trapping increases with the bulk phase solubility of the gases and with the reactivity of the solvents. These trends exemplify how interfacial and bulk liquid phenomena may track one

another. The effects of liquid temperature provide a counter-example: while thermal accommodation increases with temperature, gas solubility often decreases with T_{liq} .²³ These opposing trends emphasize the separate roles of the positive $T\Delta S(l \rightarrow g)$ term in gas–liquid solvation, which shifts equilibrium toward the gaseous state at higher temperature, and of the increasing disorder in the interface, which enhances multiple collisions and interfacial trapping of incoming gas phase atoms.

Acknowledgment. Financial support was provided by NSF Grant CHE-9417909 (G.M.N.) and by the Ballistic Missile Defense Organization/Innovative Science and Technology Office (T.K.M.). T.K.M. and G.M.N. first met as graduate student and postdoctoral fellow, respectively, in Professor Y. T. Lee's laboratory in 1985. We thank Professor Lee for his patience and dedication in training us in chemical research, for sharing his insights into the fundamental mechanisms of chemical reactions, and for his enthusiastic support of our careers.

References and Notes

- (1) King, M. E.; Nathanson, G. M.; Hanning-Lee, M. A.; Minton, T. K. *Phys. Rev. Lett.* **1993**, *70*, 1026.
- (2) Hurst, J. E.; Becker, C. A.; Cowin, J. P.; Janda, K. C.; Wharton, L.; Auerbach, D. J. *Phys. Rev. Lett.* **1979**, *43*, 1175.
- (3) Rettner, C. T.; Schweizer, E. K.; Mullins, C. B. *J. Chem. Phys.* **1989**, *90*, 3800.
- (4) Harris, J. In *Dynamics of Gas-Surface Interactions*; Rettner, C. T., Ashfold, M. N. R., Eds.; Royal Society of Chemistry: Cambridge, 1991; p 1.
- (5) King, M. E.; Saecker, M. E.; Nathanson, G. M. *J. Chem. Phys.* **1994**, *101*, 2539.
- (6) *Krytox Vacuum Pump Fluids*; Du Pont Company: Wilmington, DE; Madison, N. L.; Koo, G. P. *Fluoropolymers*; Wall, L. A., Ed.; Wiley: New York, 1972; Chapters 7 and 16. Reed, T. M. *Fluorine Chemistry*; Simons, J. H., Ed.; Academic Press: New York, 1964, Vol. V, Chapter 2.
- (7) Pradeep, T. *Chem. Phys. Lett.* **1995**, *243*, 125. Ramasamy, S.; Pradeep, T. *J. Chem. Phys.* **1995**, *103*, 485. Pradeep, T.; Miller, S. A.; Cooks, R. G. *J. Am. Soc. Mass Spectrosc.* **1993**, *4*, 769.
- (8) Lednovich, S. L.; Fenn, J. B. *AIChE J.* **1977**, *23*, 454.
- (9) Saecker, M. E.; Nathanson, G. M. *J. Chem. Phys.* **1993**, *99*, 7056.
- (10) Ronk, W. R.; Kowalski, D. V.; Manning, M.; Nathanson, G. M. *J. Chem. Phys.* **1996**, *104*, 4842.
- (11) The shoulder may also be enhanced by the ± 22 kJ/mol width of the incident beam.
- (12) See ref 5 and King, M. E. Ph.D. Thesis, University of Wisconsin, 1994 for detailed analyses of the temperature dependence of the TD flux. The TD component is fit best by temperatures equal to or slightly higher than T_{liq} when the IS and TD channels are cleanly separable.
- (13) Atoms which undergo extensive energy loss but do not fully accommodate before departing may also be classified in a "quasitrapping–desorption" channel. See: Head-Gordon, M.; Tully, J. C.; Rettner, C. T.; Mullins, C. B.; Auerbach, D. J. *J. Chem. Phys.* **1991**, *94*, 1516. Rettner, C. T.; Mullins, C. B.; Bethune, D. S.; Auerbach, D. J.; Schweizer, E. K.; Weinberg, W. H. *J. Vac. Sci. Technol. A* **1990**, *8*, 2699. Mullins, C. B.; Rettner, C. T.; Auerbach, D. J.; Weinberg, W. H. *Chem. Phys. Lett.* **1989**, *163*, 111.
- (14) This procedure is only roughly applicable to the data in Figure 7, since the TD values drop slightly with increasing θ_f . This decline may be due to an incomplete removal of the low-energy inelastic scattering from the TD channel, particularly at small θ_f .
- (15) Lipkin, N.; Gerber, R. B.; Moiseiv, N.; Nathanson, G. M. *J. Chem. Phys.* **1994**, *100*, 8408.
- (16) Tully, J. C. *J. Chem. Phys.* **1990**, *92*, 680.
- (17) Amirav, A.; Cardillo, M. J.; Trevor, P. L.; Lim, C.; Tully, J. C. *J. Chem. Phys.* **1987**, *87*, 1796 and 1808.
- (18) Benjamin, I.; Wilson, M. A.; Pohorille, A.; Nathanson, G. M. *Chem. Phys. Lett.* **1995**, *243*, 222.
- (19) Fiehrer, K. M.; Nathanson, G. M. *J. Am. Chem. Soc.* **1997**, *119*, 251.
- (20) M. Manning and G. Nathanson, to be published. We have observed that out of plane and backward scattering each grow with T_{liq} in collisions of argon atoms with liquid indium.
- (21) Harris, J. G. *J. Phys. Chem.* **1992**, *96*, 5077.
- (22) Iida, T.; Guthrie, R. I. L. *The Physical Properties of Liquid Metals*; Oxford: New York, 1993; Chapter 5.
- (23) For xenon in perfluoroalkanes, see: Kennan, R. P.; Pollack, G. L. *J. Chem. Phys.* **1988**, *89*, 517.